THE JOURNAL OF PHYSICAL CHEMISTRY B

ARTICLE

pubs.acs.org/JPCB

Heterogeneity of the Local Structure in Sub- and Supercritical Ammonia: A Voronoi Polyhedra Analysis

A. Idrissi*[,†] and I. Vyalov[†,‡]

[†]Laboratoire de Spectrochimie Infrarouge et Raman (UMR CNRS A8516), Université des Sciences et Technologies de Lille, 59655 Villeneuve d'Ascq Cedex, France

M. Kiselev[‡]

[‡]Institute of Solution Chemistry of the Russian Academy of Sciences, Akademicheskaya st. 1, 153045 Ivanovo, Russia

M. V. Fedorov[§]

[§]Max Planck Institute for Mathematics in the Sciences, D 04103 Leipzig, Germany

P. Jedlovszky[∥]

[∥]Laboratory of Interfaces and Nanosize Systems, Institute of Chemistry, Eötvös Loránd University, Pázmány P. stny 1/A, H-1117 Budapest, Hungary, HAS Research Group of Technical Analytical Chemistry, Szt. Gellért tér 4, H-1111 Budapest, Hungary, and EKF Department of Chemistry, Leányka u. 4, H-3300 Eger, Hungary

ABSTRACT: We report results of molecular dynamics simulations and detailed analysis of the local structure of sub- and supercritical ammonia in the range of temperature between 250 and 500 K along the 135 bar isobar. This analysis is based on the behavior of distributions of metric and topological properties of the Voronoi polyhedra (VP). We show that by increasing the temperature, the volume, surface, and face area distributions of the Voronoi polyhedra as well as the vacancy radius distribution broaden, particularly near the temperature T_ω, where the calculated thermal expansion coefficient has its maximum. Furthermore, the rate of increase of the corresponding mean values and fluctuations increases drastically when approaching T_α. This behavior clearly indicates that the local structure, as described by the VP, becomes increasingly heterogeneous upon approaching this temperature. This heterogeneous distribution of ammonia molecules is traced back to the increase of the large voids with increasing temperature, and is also clearly seen in the behavior of the fluctuation of the local density, as measured by the VP. More interestingly, the maximum in the heterogeneity coincides with the maximum of the fluctuation in the density of the VP.

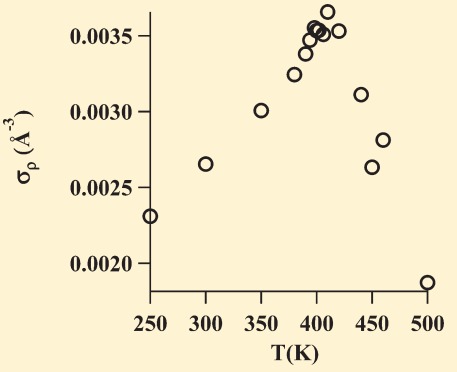

I. INTRODUCTION

One of the most important properties of supercritical fluids (SCFs) is the drastic increase of the thermodynamic response functions (e.g., thermal expansion, compressibility, heat capacity) near the critical point. As a consequence, the properties of supercritical fluids can be varied continuously from gaslike to liquidlike values by small changes in the pressure or/and temperature. This feature makes SCFs attractive alternatives to liquid solvents for use in the development of new chemical processes. From the microscopic point of view, the increase of the response functions near the critical point is associated with the heterogeneous character of the distribution of the local density. The information on the local structure is then indispensable for understanding the precise structural changes when the thermodynamic states are close to the critical point. In several previously reported experimental and theoretical studies, the importance of the local density inhomogeneity in the determination of SCF properties has been clearly underlined.[1−3] The main problem is that independent physical techniques that can give direct characterization of such inhomogeneity are not available. Indeed, although the radial distribution function, being one of the most widely used tools to investigate the local structure, gives important information on the structure of supercritical fluids, this statistical property is too much averaged to be able to describe in detail the changes of the local structure.

In characterizing the local environment of the molecules when the temperature and/or the pressure is varied, the analysis of their Voronoi polyhedra (VP) is an efficient tool. VP is the generalization

Received: May 3, 2011
Revised: June 22, 2011
Published: July 18, 2011

of Wigner−Seitz cells of crystals for disordered structures.[4] The VP of a given molecule is the locus of the spatial points that are closer to this selected molecule than to any other molecule. The geometry (i.e., shape, volume, etc.) of the polyhedron belonging to a given molecule in a liquid rapidly fluctuates due to molecular motion. The distributions of the metric and topological properties of these polyhedra can be calculated in simulations, and their shape, the position of its maximum, and their width give insight into the local molecular structure. The use of VP was suggested earlier by Finney[5,6] to analyze the topology of the local structure. Since then several publications have appeared in the literature, and the local structure of various disordered systems, such as hard spheres,[7−11] Lennard-Jones liquids,[12−16] molten[17,18] and hydrated salts,[19] liquid metals,[20−25] glass-forming liquids,[26] water[27−36] under different thermodynamic conditions, including supercritical[30,37] and supercooled states,[33,37,38] other hydrogen bonding liquids,[30] grafted[39] and soft polymers,[40] hydrated phospholipid membranes,[41] and colloidal particle packing[40−43] have been successfully characterized by means of VP analysis. It should also be noted that the VP analysis has numerous applications in other fields of sciences[4] from biophysics[36] to astrophysics[44] and from neurosciences[45] to bioinformatics.[46,47]

In the present study the local structure of ammonia is investigated in detail on the basis of long molecular dynamics (MD) calculations, performed under both sub- and supercritical conditions at temperatures ranging from 250 to 500 K along the 135 bar isobar. The topological and metric properties of VP, such as the number of the faces, face area, and volume of the polyhedron, have been quantified. The effect of increasing temperature on the shape, width, and intensity of the associated distributions allows quantifying, on the molecular level, the local structural changes accompanying the approaching and crossing the critical point of ammonia.

This paper is organized as follows. In section II, details on the performed calculations are given. In section III, the analysis of the obtained VP results is discussed in detail, whereas in section IV the conclusions drawn are given.

II. COMPUTATIONAL DETAILS

A. Molecular Dynamics Simulation. Molecular dynamics simulations have been performed on the isothermal−isobaric (N, p, T) ensemble along the 135 bar isobar, using a cubic simulation box consisting of 864 ammonia molecules under periodic boundary conditions. The potential model of ammonia proposed by Kristof et al. was used.[48] In our previous work[49] we have shown that there is good agreement between the calculated values, such as the density,[50] liquid−gas coexistence curve, thermal expansion,[50] and diffusion coefficient,[51] of this model and the corresponding experimental data. The interaction potential between two ammonia molecules contains two parts, namely a Lennard-Jones (LJ) term and a Coulomb term. The simulations have been performed using the DL_POLY program.[52] The temperature and pressure of the system have been kept constant by means of the weak coupling algorithms of Berendsen,[53] using the coupling parameter values of 0.1 ps (temperature) and 0.5 ps (pressure). All site−site interactions have been truncated to zero beyond the center−center cutoff distance of 14.5 Å. The long-range part of the electrostatic interactions has been accounted for using the Ewald summation method implemented in the DL_POLY package.[54] The equations of motion have been integrated using the leapfrog algorithm, employing an integration time step of 1.0 fs. A typical simulation run was composed of two stages: first, the system was equilibrated during 5 ns at a given temperature and pressure; second, the trajectory of particles was saved at every 10 fs during the 500 ps long production run.

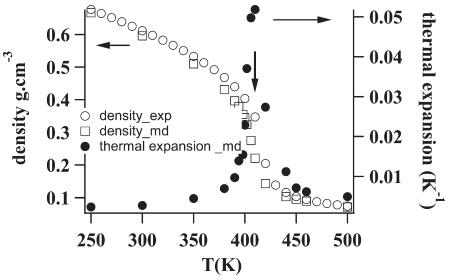

Figure 1. Experimental (open circles) and simulated (open squares) liquid−vapor coexistence curves of ammonia along the 135 bar isobar. The thermal expansion coefficients obtained in the present MD simulations by numerical differentiation of the $V(T)$ data along this isobar are also shown (filled circles). The maximum of the thermal expansion coefficient occurs at T_α = 410 K.

Seventeen temperatures, ranging from 250 to 500 K have been chosen along the 135 bar isobar. These thermodynamic states as well as the experimental coexistence curve are shown in Figure 1. The filled circles of Figure 1 show the thermal expansion coefficient, calculated by numerical differentiation of the $V(T)$ function at the 135 bar isobar. The maximum of the calculated thermal expansion coefficient occurs at T = 410 K. Throughout this paper this temperature is referred to as T_α.

B. Voronoi Polyhedra Analysis. In this study the coordinates of nitrogen atoms have been considered to be the representative points of the ammonia molecules in order to construct the VP. The VP of a given molecule is the region of space containing all the spatial points that are closer to this molecule than to any other one. The tessellation of the VP is constructed by partitioning the space around the molecules into N polyhedra, formed by the planes bisecting the sections connecting the molecules with their nearest neighbors. The VP of the molecules can be characterized by the number of its edges (N_E), vertices (N_V), and faces (N_F), the area of its individual faces (A), its total surface area (S), volume (V), and reciprocal volume, characterizing the local density around the molecules, ρ. The first three of these properties are typical topological characteristics, while the last four are the most widely used metric properties. Further, the VP vertices are the locations of the largest empty spheres (spherical vacancies) present between the molecules. These vacancies can be characterized by their radius R, which is the distance of the given vertex from the central molecule of the VP. These properties are characterized here by their full statistical distributions as well as by the mean values and standard deviations of these distributions. The distribution, mean value, and standard deviation of the quantity X are denoted here as $P(X)$, $\langle X\rangle$, and σ_X, respectively.

III. RESULTS AND DISCUSSION

A. Distribution of Various VP Properties. We computed the distribution of several VP properties, including the reciprocal volume, characteristic of the local density (ρ), volume (V), total surface area (S), area of the individual faces (A), number of faces

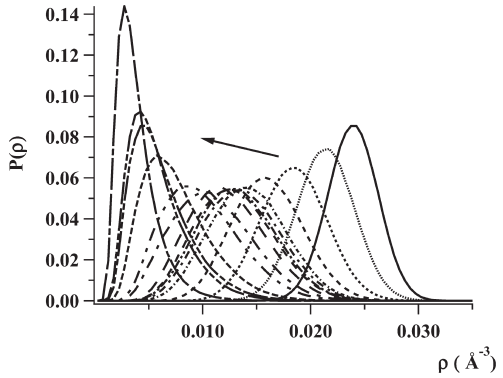

Figure 2. Density distribution of the VP of the ammonia molecules, as obtained along the 135 bar isobar at various temperatures in the range between 250 and 500 K. The arrow indicates the increase of the temperature.

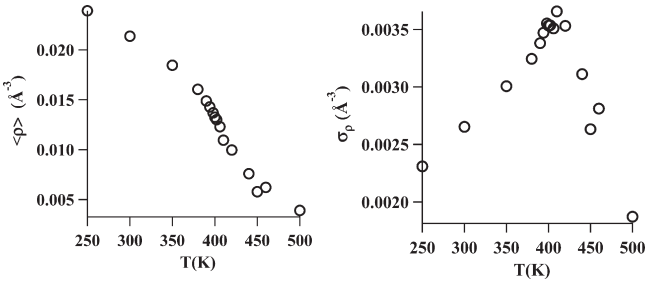

Figure 3. Mean value of the reciprocal VP volume, characterizing the local density $\langle\rho\rangle$ (left) and the corresponding standard deviation σ_ρ (right) of the $P(\rho)$ distribution as a function of the temperature.

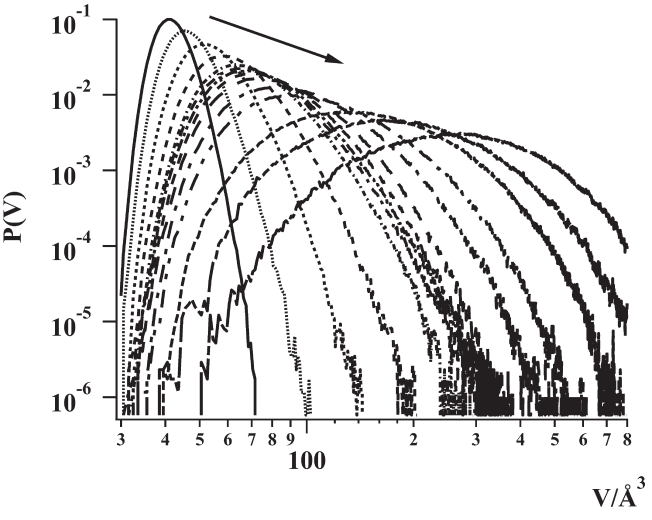

Figure 4. Volume distribution of the VP of ammonia molecules, as obtained along the 135 bar isobar at various temperatures in the range between 250 and 500 K. The arrow indicates the increase of the temperature.

(N_F), and radius of the empty spheres, centered at the VP vertices (R).

Figure 2 illustrates the change in the VP density distribution $P(\rho)$ with increasing temperature between 250 and 500 K along the 135 bar isobar. At low temperatures, far from T_α, $P(\rho)$ has a well-defined peak. As the temperature increases, (i) this peak shifts to lower values, (ii) it broadens, and (iii) the corresponding intensity decreases. Finally, as the temperature increases above T_α, the $P(\rho)$ distribution becomes significantly narrower and, at the same time, the intensity increases substantially. The dependence of the average density, $\langle\rho\rangle$, and the corresponding standard deviation, σ_ρ, on the temperature is shown in Figure 3. It is clearly seen that the rate of decrease of $\langle\rho\rangle$ increases drastically when the temperature is around 390 K. Further, the standard deviation, σ_ρ, goes through a maximum near the temperature of 410 K, i.e., T_α. This behavior clearly indicates that the local density, as described by the VP reciprocal volume, becomes increasingly inhomogeneous upon approaching the T_α temperature, and it becomes less inhomogeneous when the temperature increases above T_α.

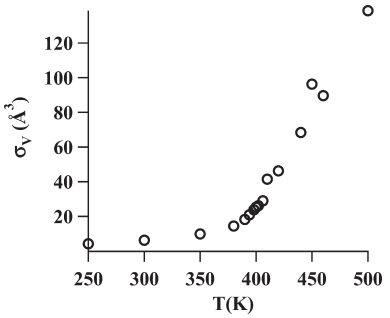

Figure 5. Standard deviation σ_V of the volume of the VP distribution as a function of the temperature.

Figure 4 shows the behavior of the VP volume distribution, $P(V)$. At low temperatures, the distribution of $P(V)$ is rather sharp around the mean volume value. With increasing temperature the distribution broadens and its peak shifts to higher volume values. Furthermore, an asymmetric tail develops on the large volume side of the $P(V)$ distribution peak, particularly near T_α. As has been explained in many previous works, the asymmetry of $P(V)$ is a consequence of the fact that in inhomogeneous systems there is no upper limit for the maximum volume of VP, while this quantity has a lower limit due to the excluded volume interaction.[13] Thus, the presence of such a long, exponential-like tail is a clear sign of inhomogeneous distribution of the molecules.[55] A quantity of interest is thus the standard deviation of this distribution, σ_V, since it measures the amplitude of the VP volume fluctuation. The behavior of σ_V has been reported as a function of the temperature in Figure 5. It shows that the rate of increase of the fluctuation in the VP volume increases drastically when the temperature is close to T_α. This behavior can be interpreted as a microscopic change, occurring at the molecular level, which results in increased thermal expansion. The physical picture emerging from this finding is that some of the geometric neighbors (i.e., the ones sharing a common VP face) with the central ammonia molecule are located, due to their increasing thermal motion, at larger distances from the central molecule, which leads to an increasing thermal expansion of the system.

The volume of a VP is closely related to the area and number of its faces. Therefore, here we analyze also the behavior of the corresponding distributions in order to get more insight into the change of the local structure of ammonia along the thermodynamic path chosen in our study. The first property characterizing the local structure around the ammonia molecules is the $P(N_F)$ distribution of the number of VP faces, which is given in

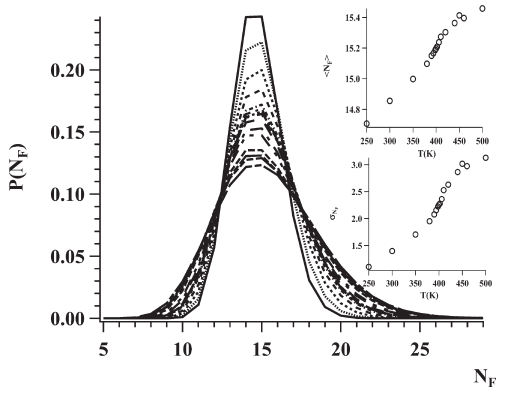

Figure 6. Number of faces distribution of the VP of ammonia molecules, as obtained along the 135 bar isobar at various temperatures in the range between 250 and 500 K. The mean value $\langle N_F \rangle$ and the corresponding standard deviation σ_{N_F} of the $P(N_F)$ distribution are given in the upper and lower insets, respectively, as a function of the temperature.

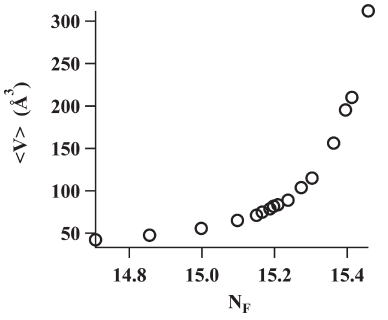

Figure 7. Correlation between average VP volume, $\langle V \rangle$, and average number of VP faces, $\langle N_F \rangle$.

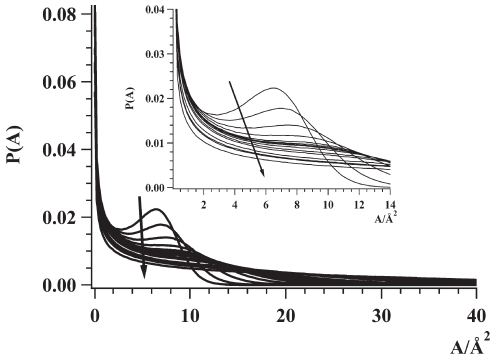

Figure 8. Face area distribution of the VP, as obtained along the 135 bar isobar at various temperatures in the range between 250 and 500 K. The inset shows the region of the second, nontrivial peak on a magnified scale. The arrows indicate the increase of temperature.

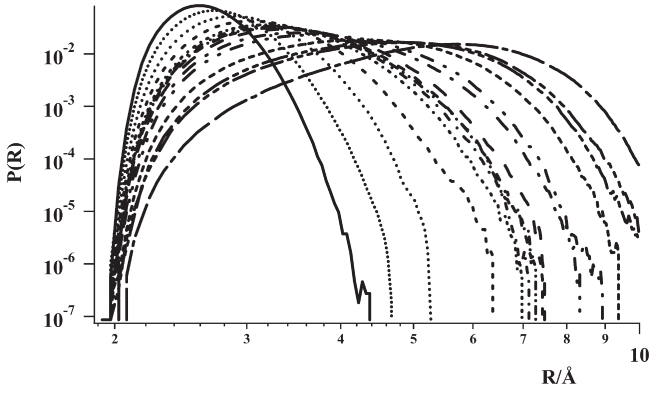

Figure 9. Distribution of the radius of the spherical voids present in ammonia, as obtained along the 135 bar isobar at various temperatures in the range between 250 and 500 K. The two axes are on logarithmic scale.

Figure 6. The mean number of the face area of the VP resulted in around 14.7 at the lowest temperature and around 15.5 at the highest temperature considered (see the upper inset of Figure 6), can be interpreted as the number of geometric neighbors of each ammonia molecule. It should be mentioned that in the present work the faces are not weighted by their area, which is probably the main reason for the misleading occurrence of large values in such distributions.[56−58] Indeed, the distance of the 15th nearest neighbor from the central molecule is clearly larger than the position of the first minimum of the nitrogen−nitrogen radial distribution function, which defines the spatial extent of the first coordination shell. This confirms that the behavior of the VP face number distribution is shaped by the neighbor molecules located at distances beyond the first coordination shell. We notice a drastic decrease of the intensity of the maximum and some broadening of the $P(N_F)$ distribution as the temperature increases. Further, the $P(N_F)$ distributions are more skewed toward large values of N_F at the higher temperatures. This increase of the contribution of large N_F values to the total $P(N_F)$ distribution can be interpreted as a sign of the geometric rearrangement of distant neighbors when the temperature increases. Indeed, the large fluctuation of the position of the farthest neighbors forming the polyhedra (distant neighbors will cease to be neighbors if their positions are slightly perturbed) induces an increase of the fluctuation in the number of faces. The correlation between the average volume of the VP and the average number of its faces is illustrated in Figure 7. As is clearly seen, at temperatures near T_α a small change in the value of $\langle N_F \rangle$ is accompanied by large changes in the mean VP volume.

The second parameter that helps to characterize the VP properties is the distribution of the area of its faces, $P(A)$. The behavior of this distribution is illustrated in Figure 8. At low temperatures there are two peaks in the face area distribution $P(A)$. The first, high, trivial peak around the surface area value of 0 is given by the large number of distant neighbors, sharing only tiny VP faces with the central molecule.[21] This peak is rather insensitive to the temperature and provides no information on the local arrangement of the molecules around each other. The second peak is located at higher values of the face area distribution. The position of this peak shifts slightly toward higher face area values and gradually flattens out as the temperature approaches T_α. The change in the intensity of the second peak of $P(A)$ results from the change of the number of closest neighbor molecules.[10] Furthermore, the distance between two vertices of the VP face must be larger than a certain minimum value due to the excluded volume (repulsive interaction) of the corresponding neighbor molecules. It is therefore logical to expect that this peak would be much narrower and sharper at low temperatures (small fluctuation of the position of the neighboring molecules that determine the VP). The shift and flattening of this peak are associated with the increase of the

dx.doi.org/10.1021/jp204078u |J. Phys. Chem. B 2011, 115, 9646–9652

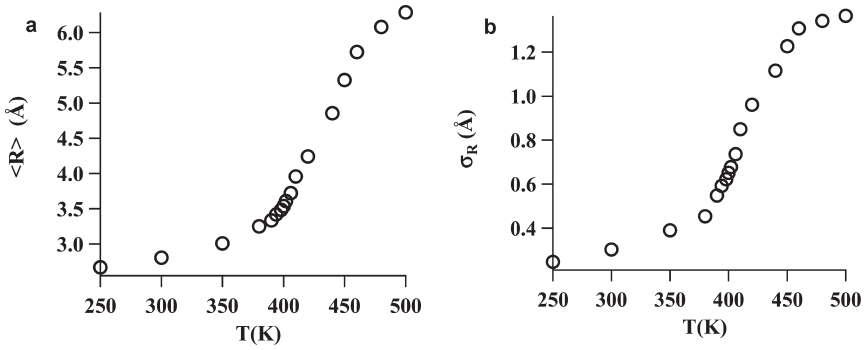

Figure 10. Behavior of (a) the void radius average distance and (b) the corresponding fluctuation as a function of temperature.

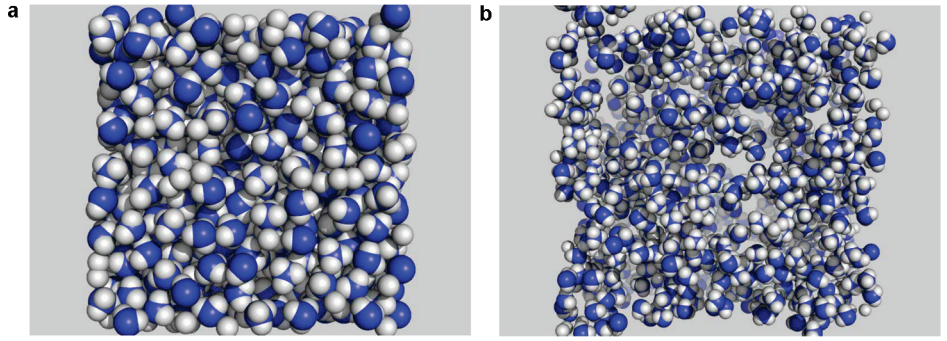

Figure 11. Equilibrium snapshots of ammonia, as taken from the simulations performed at (a) T = 250 K and (b) T = 420 K.

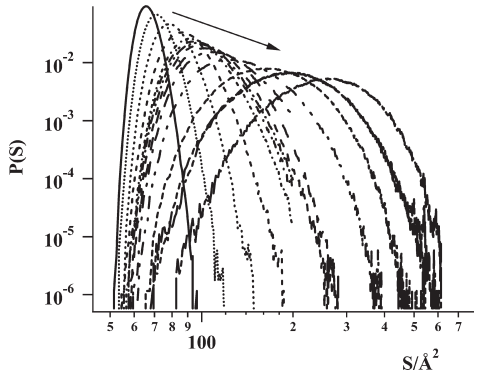

Figure 12. Distribution of the total surface area of the VP distributions, as obtained along the 135 bar isobar at various temperatures in the range between 250 and 500 K. The arrow indicates the increase of the temperature. The two axes are on logarithmic scale.

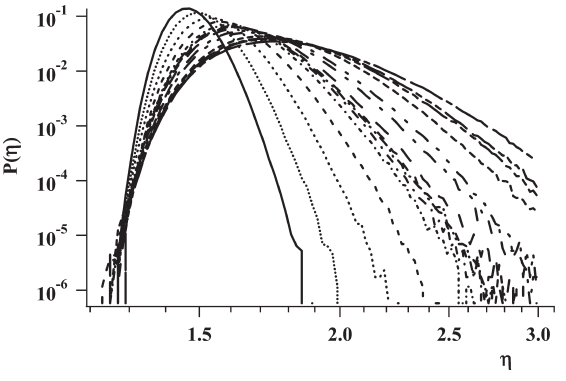

Figure 13. Distribution of the asphericity parameter of the VP, as obtained along the 135 bar isobar at various temperatures in the range between 250 and 500 K.

distance of some vertices belonging to this face from the central molecule due to the thermal expansion of the system. This information can also be obtained from the behavior of the vacancy radius $P(R)$ distribution, which is illustrated in Figure 9. $P(R)$ has a well-defined peak at low temperatures (i.e., high densities). When the temperature increases above T_α the intensity of the distribution reduces substantially, and a concomitant broadening of the distribution and a shift of its peak to higher R values are observed. All these changes can be associated with the formation of large voids. The increase of temperature leads to an increase of the average void size, as $\langle R \rangle$ shifts upward large values. The rate of increase of $\langle R \rangle$ becomes particularly high near the temperature T_α (see Figure 10a). The local structure responds to an increase of the temperature by creating large voids, the distribution of which becomes increasingly heterogeneous, as indicated by the increase of its fluctuation σ_R (see Figure 10b). These results support the physical picture that the maximum of the thermal expansion coefficient is associated with the transition from the situation when small voids of rather uniform size dominate the $P(R)$ distribution to that when rather large voids also appear besides these small, uniformly sized ones. The observed increase of the void radius is also illustrated by Figure 11, showing equilibrium snapshots of ammonia as taken

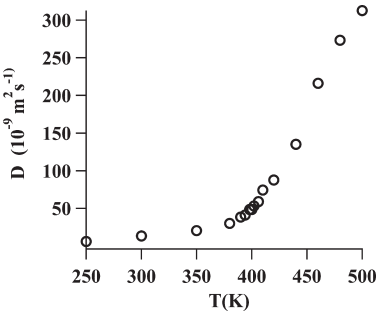

Figure 14. Diffusion coefficient of ammonia as function of temperature.

from the simulations performed at the temperatures of $T = 250$ K and $T = 420$ K, respectively.

As there is a strong correlation between the volume and the total surface area (S) of the VP, the same qualitative behavior is found for the $P(S)$ distribution as what was also observed for $P(V)$. Indeed, at low temperatures, the $P(S)$ distribution is peaked around the mean surface area value (see Figure 12). As the temperature increases, we notice a decrease of the intensity of the maximum of $P(S)$ and a concomitant shift and broadening of this peak. The behavior of $\langle S \rangle$ and σ_S with increasing temperature is similar to that of $\langle V \rangle$ and σ_V in the sense that a change in the rate of increase of the mean value of both parameters as well as a maximum of both standard deviations can be noticed when the temperature is close to T_α. The information concerning the change in the volume and the surface of the VP may be gathered in the asphericity parameter, which combines volume and surface area into a single descriptor to measure how far the shape of the polyhedron is from that of a perfect sphere. The asphericity parameter, defined as[30]

$$\eta = \frac{S^3}{36\pi V^2}$$

approaches unity if the VP is less distorted in its shape (the three principal axes of the VP have almost equal length); otherwise it is considerably larger than unity. Therefore, the asphericity parameter can be used to characterize the VP anisotropy. At low temperatures, the distribution is defined by a narrow and symmetric peak, centered at around 1.51 (see Figure 13). As the temperature increases, $P(\eta)$ shifts to higher values with a concomitant decrease of its intensity and a broadening of its shape. The largest gradient of the average value of the asphericity parameter as function of temperature is observed around T_α.

B. Diffusion Coefficient and the VP Analysis. The changes in the topological properties of the system with increasing temperature are expected to lead to changes also in several physical properties. In the following, we discuss the correlation between the local structure, as revealed by the VP analysis, and a macroscopic property, namely the diffusion coefficient, D, the temperature dependence of which along the 135 bar isobar is illustrated in Figure 14. The diffusion coefficients have been calculated from the mean square displacement. The rate of increase of D undergoes a drastic change near the temperature T_α. One can expect that the dynamics of a single molecule is largely determined by its nearest neighbors, the spatial distribution of which is described by the VP properties. Indeed, our results suggest that as far as small VP volumes and small vacancy radii dominate their respective total distributions, the large number of nearby neighbors imposes a strong caging effect, which reduces the diffusion of the molecules. The increasing temperature has a "softening" effect on these cages formed by the nearest neighbors, and at higher temperatures the cage should even disappear, indicating a translational diffusion regime. The softening of the cage is associated with the observed increase of the VP volumes and radii of the spherical voids among the molecules. This results in a change of the rate of increase of the diffusion coefficient, as seen from Figure 14.

IV. CONCLUSIONS

We have reported results of a statistical analysis of Voronoi polyhedra in sub- and supercritical ammonia in a wide temperature range, between 250 and 500 K, along the 135 bar isobar. Typical topological and metric properties have been quantified as functions of the temperature. Our results led to the following main conclusions.

(i) The distributions of the VP volume and total surface area, and of the radius of the spherical voids located at the VP vertices, are characterized by a single peak at low temperatures, and as the temperature increases, these distributions increasingly broaden, in particular, near T_α (i.e., where the maximum of the thermal expansion coefficient occurs). This behavior is interpreted as a signature of the inhomogeneity of the spatial distribution of the ammonia molecules.

(ii) The inhomogeneity of the spatial distribution of the ammonia molecules is strongly correlated with the change in the rate of increase of the average value of the VP volume, surface area, area, and number of the individual VP faces, and radius of the spherical voids between the molecules.

(iii) The behavior of some macroscopic properties, such as the diffusion coefficient, is strongly correlated with changes in the local structure. Indeed, for temperatures below T_α the local structure is characterized by the dominance of small and rather uniform values contributing to the respective distributions of the VP volume and surface area as well as of the void radius. The dominance of these small values is associated with the occurrence of the strong caging effect of the nearest neighbors, which results in relatively small values of the diffusion coefficient. As the temperature increases, the contribution of large values to these distributions becomes gradually dominant, in accordance with a softening of the cage formed by the neighboring molecules, which correlates with the observed drastic increase of the diffusion coefficient.

AUTHOR INFORMATION

Corresponding Author
*E-mail: nacer.idrissi@univ-lille1.fr.

ACKNOWLEDGMENT

P.J. thanks the LASIR laboratory of the USTL University, Lille, for its hospitality. The Institut du Développement et des Ressources en Informatique Scientifique, the Centre de Ressources Informatiques (CRI) de l'Université de Lille, and the Centre de Ressources Informatiques de Haute-Normandie (CRIHAN) are thankfully acknowledged for the CPU time allocation. This project was supported by the Marie Curie Program IRSES (International Research Staff Exchange Scheme, GA No. 247500) and by the Hungarian OTKA Foundation under Project No. 75328.

REFERENCES

(1) Musso, M.; Matthai, F.; Keutel, D.; Oehme, K.-L. *Pure Appl. Chem.* **2004**, *76*, 147.
(2) Tucker, S. C. *Chem. Rev.* **1999**, *99*, 391.
(3) Rovere, M.; Heermann, D. W.; Binder, K. *J. Phys.: Condens. Matter* **1990**, *2*, 7009.
(4) Okabe, A.; Boots, B.; Sugihara, K.; Chiu, S. N. *Spatial Tessellations Concepts and Applications of Voronoi Diagrams*; John Wiley &Sons, Ltd.: New York, 2000.
(5) Finney, J. L. *Nature* **1977**, *266*, 309.
(6) Finney, J. L. *Proc. R. Soc. London* **1970**, *319*, 479.
(7) Oger, L.; Gervois, A.; Troadec, J. P.; Rivier, N. *Philos. Mag. B* **1996**, *74*, 177.
(8) Lavrik, N.; Voloshin, V. P. *J. Chem. Phys.* **2001**, *114*, 9489.
(9) Sastry, S.; Truskett, T. M.; Debenedetti, P. G.; Torquato, S.; Stillinger, F. H. *Mol. Phys.* **1998**, *95*, 289.
(10) Yang, R. Y.; Zou, R. P.; Yu, A. B. *Phys. Rev. E* **2002**, *65*, 041302.
(11) Richard, P.; Oger, L.; Troadec, J. P.; Gervois, A. *Physica A* **1998**, *259*, 205.
(12) Ruff, I.; Baranyai, A.; Palinkas, G.; Heinzinger, K. *J. Chem. Phys.* **1986**, *85*, 2169.
(13) Montoro, J.; Gil, C.; Abascal, J. L. F. *J. Phys. Chem.* **1993**, *97*, 4211.
(14) Voloshin, V. P.; Naberukhin, Y. I.; Medvedev, N. N.; Jhon, M. S. *J. Chem. Phys.* **1995**, *102*, 4981.
(15) Voloshin, V. P.; Beaufils, S.; Medvedev, N. N. *J. Mol. Liq.* **2002**, *96*−*97*, 101.
(16) Yang, R. Y.; Zou, R. P.; Dong, K. J.; An, X. Z.; Yu, A. *Comput. Phys. Commun.* **2007**, *177*, 206.
(17) Baranyai, A.; Ruff, I. *J. Chem. Phys.* **1986**, *85*, 365.
(18) Pusztai, L.; et al. *J. Phys. C: Solid State Phys.* **1988**, *21*, 3687.
(19) Montoro, J.; Gil, C.; Bresme, F.; Abascal, J. L. F. *J. Chem. Phys.* **1994**, *101*, 10892.
(20) Luchnikov, V. A.; Medvedev, N. N.; Appelhagen, A.; Geiger, A. *Mol. Phys.* **1996**, *88*, 1337.
(21) Brostow, W.; Chybicki, M.; Laskowski, R.; Rybicki, J. *Phys. Rev. B* **1998**, *57*, 13448.
(22) Hoare, M. R. *J. Non-Cryst. Solids* **1978**, 31.
(23) Aparicio, N. D.; Cocks, A. C. F. *Acta. Metall. Mater.* **1995**, 43.
(24) Maruyama, K.; Endo, H.; Hoshino, H.; Hensel, F. *Phys. Rev. B* **2009**, *80*, 014201.
(25) Hoyer, W.; Kleinhempel, R.; Lorinszi, A.; Pohlers, A.; Sava, F. *J. Phys.: Condens. Matter* **2005**, *17*, S31.
(26) Starr, F. W.; Sastry, S.; Douglas, J. F.; Glotzer, S. C. *Phys. Rev. Lett.* **2002**, *89*, 125501.
(27) Ruocco, G.; Sampoli, M.; Vallauri, R. *J. Chem. Phys.* **1992**, *96*, 6167.
(28) Ruocco, G.; Sampoli, M.; Torcini, A.; Vallauri, R. *J. Chem. Phys.* **1993**, *99*, 8095.
(29) Shih, J.-P.; Sheu, S.-Y.; Mou, C.-Y. *J. Chem. Phys.* **1994**, *100*, 2202.
(30) Jedlovszky, P. *J. Chem. Phys.* **2000**, *113*, 9113.
(31) Yeh, Y.; Mou, C.-Y. *J. Phys. Chem. B* **1999**, *103*, 3699.
(32) Mountain, R. D. *J. Chem. Phys.* **1999**, *110*, 2109.
(33) Jedlovszky, P.; Partay, L. B.; Bartok, A. P.; Voloshin, V. P.; Medvedev, N. N.; Garberoglio, G.; Vallauri, R. *J. Chem. Phys.* **2008**, *128*, 244503.
(34) Etzler, F. M.; Ross, R. F.; Halcomb, R. A. *Physica A* **1991**, 172.
(35) Rapaport, D. C. *Mol. Phys.* **1983**, *48*, 23.
(36) Soyer, A.; Chomilier, J.; Mornon, J.-P.; Jullien, R.; Sadoc, J.-F. *Phys. Rev. Lett.* **2000**, *85*, 3532.
(37) Jedlovszky, P. *J. Chem. Phys.* **1999**, *111*, 5975.
(38) Okabe, I.; Tanaka, H.; Nakanishi, K. *Phys. Rev. E* **1996**, *53*, 2638.
(39) Tokita, N.; Hirabayashi, M.; Azuma, C.; Dotera, T. *J. Chem. Phys.* **2004**, *120*, 496.
(40) Sega, M.; Jedlovszky, P.; Medvedev, N. N.; Vallauri, R. *J. Chem. Phys.* **2004**, *121*, 2422.
(41) Alinchenko, M. G.; Voloshin, V. P.; Medvedev, N. N.; Mezei, M.; Pártay, L.; Jedlovszky, P. *J. Phys. Chem. B* **2005**, *109*, 16490.
(42) Schenker, I.; Filser, F. T.; Gauckler, L. J.; Aste, T.; Herrmann, H. J. *Phys. Rev. E* **2009**, *80*, 021302.
(43) Varadan, P.; Solomon, M. J. *J. Rheol.* **2003**, 47.
(44) van de Weygaert, R.; Icke, V. *Astron. Astrophys.* **1989**, *213*, 1.
(45) Ahnelt, P. K.; Fernández, E.; Martinez, O.; Bolea, J. A.; Kübber-Heiss, A. *J. Opt. Soc. Am. A* **2000**, *17*, 580.
(46) Karch, R.; Neumann, F.; Neumann, M.; Szawlowski, P.; Schreiner, W. *Ann. Biomed. Eng.* **2003**, *31*, 548.
(47) Tsai, J.; Gerstein, M. *Bioinformatics* **2002**, *18*, 985.
(48) Kristof, T.; Vorholz, J.; Liszi, J.; Rumpf, B.; Maurer, G. *Mol. Phys.* **1999**, *97*, 1129.
(49) Vyalov, I.; Kiselev, M.; Tassaing, T.; Soetens, J. C.; Idrissi, A. *J. Phys. Chem. B* **2010**, *114*, 15003.
(50) Bone, R. G. A.; Handy, N. C. *Theor. Chim. Acta* **1990**, *78*, 133.
(51) O'Reilly, D. E.; Peterson, E. M.; Scheie, C. E. *J. Chem. Phys.* **1973**, *58*, 4072.
(52) Tsuzuki, S.; Uchimaru, T.; Tanabe, K.; Kuwajima, S.; Tajima, N. *J. Phys. Chem.* **1996**, *100*, 4400.
(53) Berendsen, H. J. C.; Postma, J. P. M.; van Gunsteren, W. F.; DiNola, A.; Haak, J. R. *J. Chem. Phys.* **1984**, *81*, 3684.
(54) Anderson, H. C. *J. Comput. Phys.* **1983**, *52*, 24.
(55) Zaninetti, L. *Phys. Lett. A* **1992**, *165*, 143.
(56) Xu, T.; Li, M. *Philos. Mag.* **2009**, *89*, 349.
(57) Dong, K. J.; et al. *EPL* **2009**, *86*, 46003.
(58) Jullien, R.; et al. *Phys. Rev. E* **1996**, *54*, 6035.